

CONTRIBUTION OF US AND CT FOR DIAGNOSIS OF INTRAPERITONEAL FOCAL FAT INFARCTION (IFFI): A PICTORIAL REVIEW

B. Coulier¹

The term IFFI – for Intraperitoneal Focal Fat Infarction – includes various acute abdominal clinical conditions in which focal fatty tissue necrosis represents the common pathologic denominator. Only differing by their various anatomical locations and dimensions, all cases nevertheless present rather similar clinical signs, aetiology, radiological features and prognosis.

In clinical practise, most cases of IFFI concern torsion and/or infarction of the greater omentum or epiploic appendages. Rarer types of torsion and/or infarction of lipomatous appendages of the hepatic falciform ligament and of the lesser omentum have also been reported. Cases are finally described in the paediatric population.

US and merely CT have been shown having a high sensitivity and specificity for the diagnosis of IFFI and in most cases the clinical evolution is spontaneously favourable. For these two reasons, the option of conservative treatment after specific imaging diagnosis now represents the other common denominator of IFFI.

Such a safe and unambiguous imaging diagnosis of IFFI represents thus an important challenge for each abdominal radiologist with the intention of persuading the referent clinician to avoid unnecessary surgery for their patients.

The aim of this pictorial review is to extensively explore not only the classical imaging findings of various types of IFFI but also to review the normal US and MDCT anatomy of the fatty abdominal structures being usually implicated in IFFI. More rare or atypical presentations are also illustrated as well as subacute findings and sequels. All reported patients were collected in our department during a 7-year-period and most were successfully treated conservatively.

Key-words: Abdomen, acute conditions – Abdomen, CT – Abdomen, US.

The term IFFI – for Intraperitoneal Focal Fat Infarction – was introduced by van Breda Vriesmann in 1999 (1) to gather and qualify various acute abdominal clinical conditions having focal fatty tissue necrosis as common denominator, presenting rather similar clinical signs, aetiology, radiological features, prognosis and treatment and finally only differing in their anatomical location and dimensions.

First considered as being rare, IFFI has received much attention during the last two decades. The main reason are the continuous development of CT and US technology and their exponentially use as first line imaging modalities to explore patients presenting with acute abdominal conditions. It is now suggested that their true frequency is much higher than previously considered and numerous case reports, small series and pictorial reviews have been published on this subject.

Because the disease has been shown to have a spontaneously favourable evolution in most cases the option of successful conservative treatment has now become the other common denominator of IFFI.

A safe and unambiguous imaging diagnosis of IFFI thus currently represents a challenge for any abdominal radiologist in order to avoid unnecessary surgery.

In this large pictorial review we first revisit the normal US and CT anatomy of the fatty abdominal structures being usually implicated in IFFI. The classical but also nontypical imaging findings of IFFI are then extensively re-explored. Finally more rare or nontypical presentations are also illustrated as well as subacute findings and sequels.

All reported cases were collected in our department over a 7-year-period. The great majority of patients were imaged with MDCT and most patients were successfully treated conservatively.

Discussion

Epiploic appendages

Epiploic appendages (EA) correspond to peritoneum covered fatty fingerlike structures about 2 to 5 cm long and 1-2 cm thick (1-5). They are about 50-100 in number, arise from the serosal surface of the colon, con-

tain adipose tissue and vessels and are distributed in two parallel rows along the taenia libera and the taenia omentalis, from the cecum to the rectosigmoid junction (Fig. 1, 2). The largest are found along the descending and sigmoid colon. Those developed along the transverse colon are smaller.

It is worthwhile to note that the transverse colon usually harbours only a single row of EA along its taenia libera because the greater omentum attaches along the taenia omentalis (Fig. 3). Nevertheless isolated EA may occasionally occur at this last site as well as over the vermiform appendix or over a small bowel loop.

Their somewhat precarious terminal blood supply – one or two small colonic end-arteries and a small draining vein –, their pediculated nature and thus their great mobility are factors increasing their susceptibility for torsion and/or infarction.

The precise function of EA is not yet known but they can provide some defence against local inflammation similar to the protective properties of the greater omentum. They also represent a site for fat storage (4).

Under normal circumstances, the EA are not visible during ultrasound studies or abdominal CT unless they are surrounded by a sufficient amount of ascitic fluid (Fig. 1), free peritoneal gas or intermingled with

From: 1. Department of Diagnostic Radiology, Clinique St Luc, Bouge, Belgium.
Address for correspondence: Dr B. Coulier, M.D., Department of Diagnostic Radiology, Clinique St Luc, Rue St Luc 8, B-5004 Bouge, Belgium.
E-mail: bcoulier@skynet.be

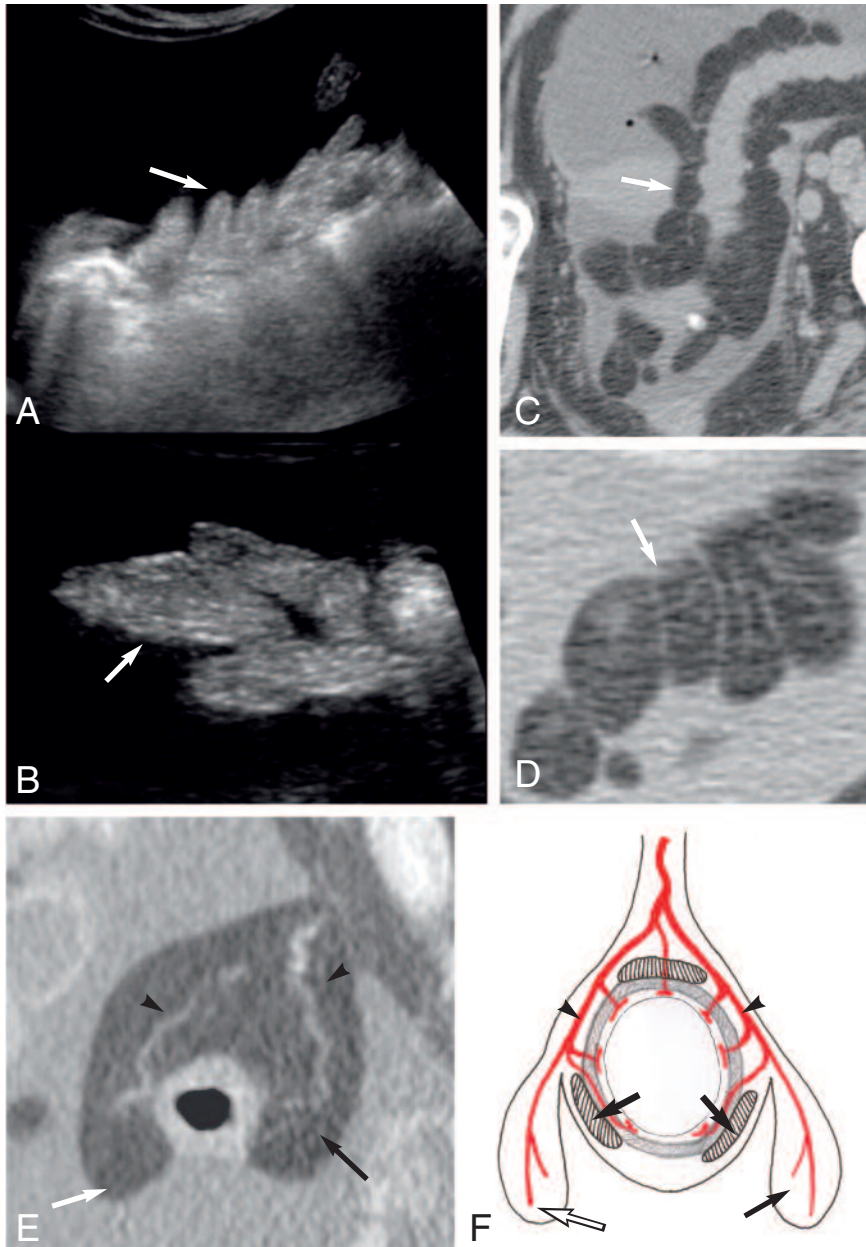


Fig. 1. — Epiploic appendages are commonly visible in patients presenting with massive ascitis. US appearance (A, B) of rows of normal epiploic appendages (white arrow) floating in ascitis in the left iliac fossa in a cirrhotic patient. Similar images (C, D) obtained during abdominal MDCT. Anatomic relation (E, F) between the appendages and the axis of the colon: two parallel rows of appendages, also well demonstrated on the coronal oblique MPR view (C) are running along the colon inserting near the anti mesenteric taenia (taenia libera –black arrow– and taenia omentalis –white arrow–). They are vascularised by secondary terminal branches of the vasa recta longa of the colon (black arrowheads).

peritoneal inflammatory processes and/or when their covering peritoneal sheet is inflamed (4) (Fig. 2).

Acute epiploic appendagitis (AEA) is an uncommon cause of abdominal pain that has only recently been recognized and whose diagnosis primarily relies on cross sectional imaging

– most often CT or US – (3). It is attributable either to torsion or to spontaneous venous thrombosis of an EA. The blood supply is cut off to the fat cells that compose the bulk of the EA, with resultant ischemia and possibly infarction. The necrosis can sometimes be haemorrhagic (Fig. 5).

Primary AEA present as an acute clinical condition which can mimic diverticulitis, appendicitis or other more serious causes of acute abdominal pain (5). The sigmoid colon and the caecum are the predominant physiological sites of occurrence but all parts of the colon may be affected. AEA can occur at any age and men are slightly more affected than women (7:3 ratio) (1, 5).

On clinical examination patients describe a localised, strong, non migratory, sharp pain which usually started after a specific physical movement of their body like post-prandial exercise (1, 5, 6). Abdominal local tenderness is present in all patients. There is a lack of fever, vomiting or other complaints. Leucocytosis is found in only about 20% of cases. Clinically it is most often mistaken for acute diverticulitis. Approximately 7,1% of patients investigated to exclude sigmoid diverticulitis have imaging findings of primary AEA (7). When it involves the caecum, it may be mistaken clinically for acute appendicitis.

In most cases primary AEA has virtually pathognomonic CT findings (Fig. 4, 5, 6), appearing as a pericolic, generally oval-shaped lesion with fat attenuation – but with higher attenuation (mean, -60HU) than uninvolved fat (mean, -120HU) –, thickened visceral peritoneal lining, and periappendageal fat stranding (8, 9). Additional CT findings may include a longitudinal linear area or a central high-attenuating dot or focus and, as well as mass effect, focal wall thickening of the adjacent colon, or both. The high density central dot or focus - found in about 54% of cases - is believed to represent a thrombosed vessel within the inflamed appendix (3).

Follow-up imaging of epiploic appendagitis are not systematically performed because of the benign nature of the lesion and the generally spontaneously healing. Nevertheless it is important to be aware of the evolutionary follow-up CT findings of acute epiploic appendagitis because these findings may persist for several months after disappearance of the clinical symptoms (3) (Fig. 7). With time the AEA decreases in size, usually to a small lesion with fat attenuation – that may become more similar to that of uninvolved mesenteric fat - but sometimes to a nugget with soft tissue attenuation that reflects scar tissue deposition (3, 9). It also change in shape and contour usually from a

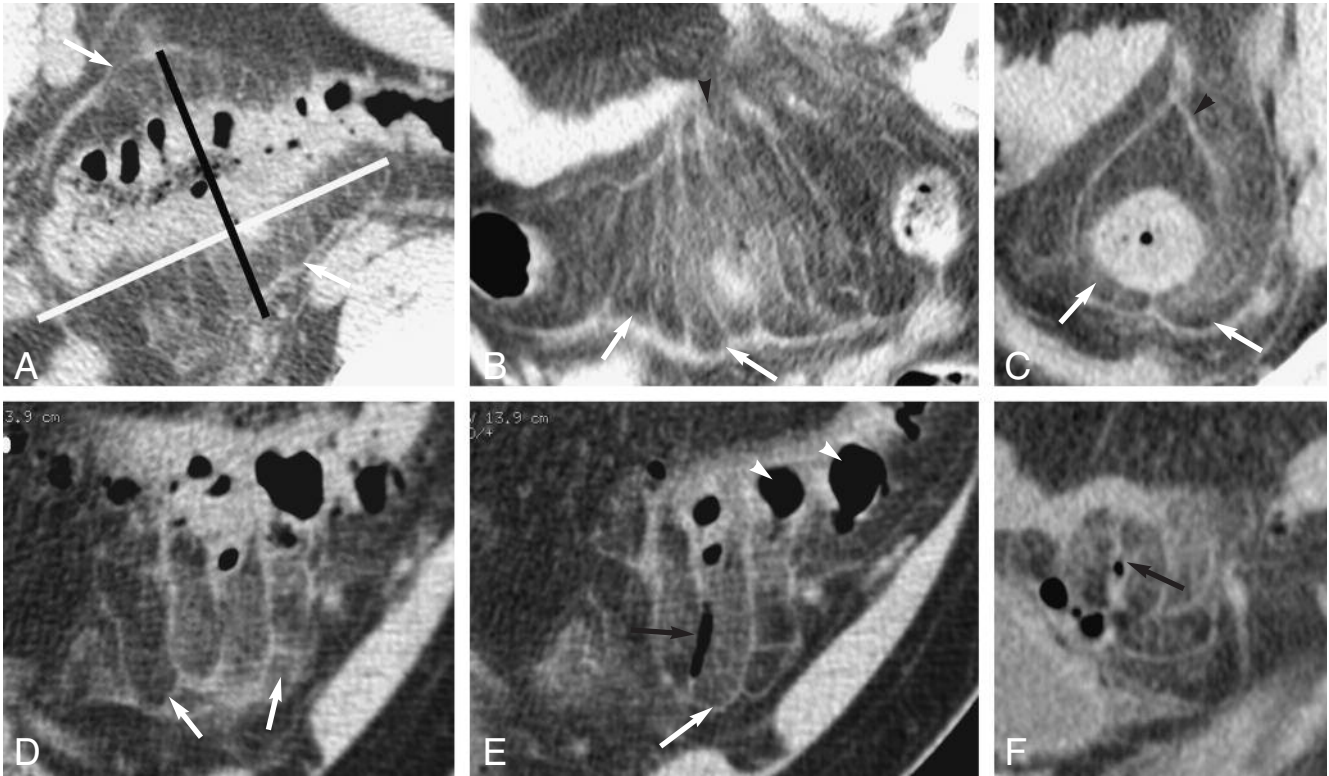


Fig. 2. — Normal epiploic appendages also appear clearly when inflammatory processes occur around them and/or when their covering peritoneal sheet is inflamed. Transverse MPR view (A), sagittal oblique MPR view (B) (along the white line) and cross section view of the sigmoid colon (C) (along the black line) show enhanced visualisation -due to peritoneal irritation- of the two parallel rows of epiploic appendages of the sigmoid colon (white arrows) in a patient presenting with colonic diverticulitis. The feeding vessels are well visible (black arrowhead). In another case or perforated diverticular sigmoiditis (D-F) the digitiform appendages (white arrows) are enhanced by the presence of fluid and irritation of the peritoneum. The vicinity between the appendages and the diverticula is also illustrated (white arrowheads). Free intraperitoneal gas due to perforation is retained between the appendages (black arrow).

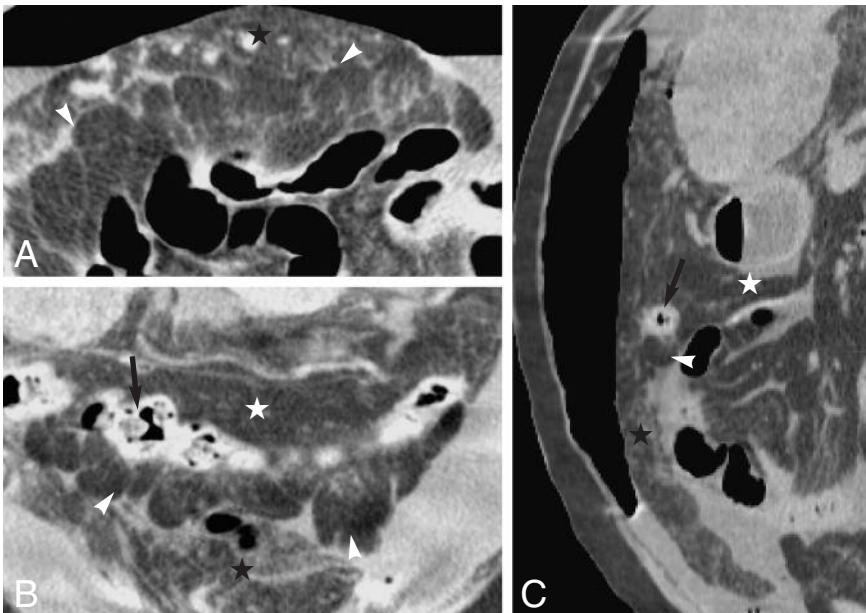


Fig. 3. — More deeply located rows of epiploic appendages are physiologically found along the internal side of the ascending colon and under the transverse colon. These may also be spontaneously seen in the presence of ascitis and/or peritoneal irritation. Transverse (A), sagittal (B) and coronal (C) MPR views in a patient presenting with massive hydro pneumoperitoneum. A continuous row of appendages (white arrowheads) are hanging along the taenia libera of the transverse colon (black arrow) and thus under the greater omentum (black star); white star = transverse mesocolon.

well-defined smooth oval shape to a structure with a shape that is irregular, oval or perfectly round. Classical fat stranding and/or adjacent bowel changes also improve around the healing appendagitis (3, 9).

In the later course, the infarcted tissue can calcify, and a detachment of the epiploic appendage may be a source of "loose intraperitoneal bodies" or "peritoneal mice" incidentally found during laparoscopy or during radiologic evaluation (5) (Fig. 8).

During ultrasound the lesion typically appears as an hyperechoic nodule of about 2 or 3 cm generally underneath the anterior abdominal wall at the site of maximum tenderness. The nodule is typically non-compressible and surrounded by a hypoechoic halo representing the inflamed peritoneum (1, 5, 9).

Falciform ligament

The falciform ligament (FL) is formed by two layers of peritoneum and contains a variable amount of extraperitoneal fat along with the remnants of the umbilical vein and

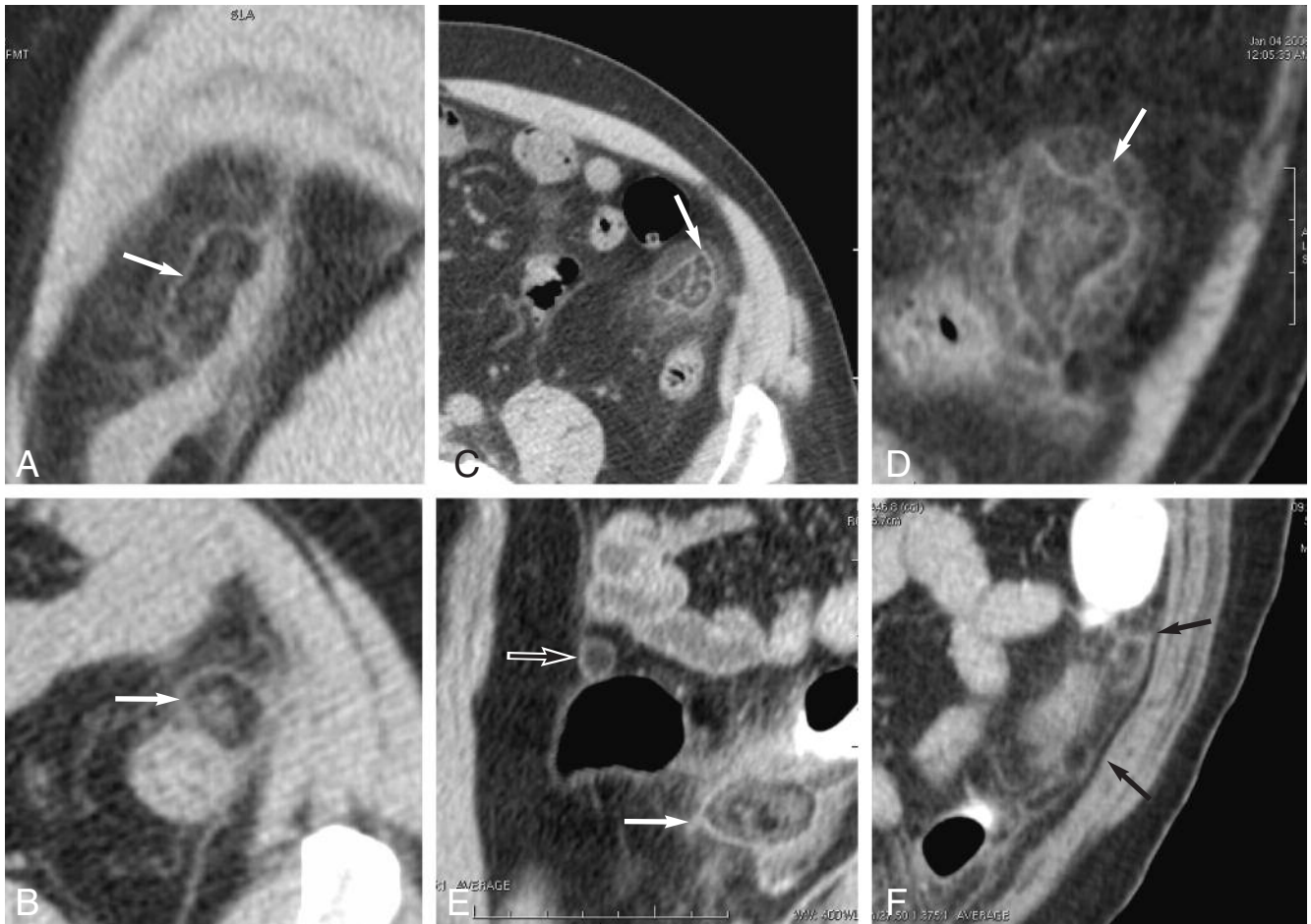


Fig. 4. — A selection of very typical CT findings in different cases of acute epiploic appendagitis (AEA): sagittal (A) and axial (B) MPR views of an AEA of the anterior portion of the descending colon. Axial (C & D) views of another AEA of the left colon. In this patient (E, F) presenting with an acute abdominal pain related to a fresh AEA (white arrow) three older atrophic infarcted appendages (black arrows) are fortuitously demonstrated.

In each case of AEA, the inflammatory necrotic lipomatous appendage measures 1,5 to 2 cm, contains dense structures probably corresponding to thrombosed vessels, appears circumscribed by a thickened inflammatory peritoneum and surrounded by a more subtle halo of inflammatory neighbouring fat tissue constituted by other EA or portions of the GO.

the ligamentum teres (10). Starting at the umbilicus in the midline, it passes to the right of the midline to connect the liver at the level of the accessory fissure.

Fatty appendages are also commonly found on the FL during coelioscopy and are occasionally spontaneously visible during abdominal CT in patients presenting with ascitis or pneumoperitoneum (Fig. 9). Except the ligamentum teres, the FL complex usually remains undistinguishable from other peritoneal and properitoneal fatty structures (11).

Surgical lesions implicating the FL are extremely uncommon and are represented by the rare internal hernia through the ligament, cystic lesions – primary congenital cysts or secondary infectious, neoplastic or

traumatic cysts – and rare extension of cholecystitis (11, 12). Lipomas of the FL are also rare described lesions (13).

Torsion of the FL or of a lipomatous appendage of the FL is a very rare cause of acute abdominal pain and only five cases have been described as separate case reports (10, 14). The presentation is very similar to omental torsion with localized peritonism without fever or elevated white cell count and the differential diagnosis has to be made essentially with cholecystitis and perforated gastroduodenal ulcer.

The US and CT appearances of a torsion of the free fatty end or of an appendage of the FL is very similar to that of AEA or omental torsion except the location. CT and particularly MPR is obvious for adequately

identifying the lesion as separate from the surrounding structures (10) and US may be useful to demonstrate the fact that the lesion doesn't move with breathing, thereby proving its superficial extraperitoneal nature (14) (Fig. 9).

All published cases have been operated but it should be suggested that a better knowledge and thus a better recognition of the entity could also avoid unnecessary surgery.

Greater omentum

Anatomically, the GO is a large free-hanging mesenteric tissue apron arising from the greater gastric curvature, crossing the transverse colon and descending in front of the viscera down to the symphysis (15, 16). After a distance

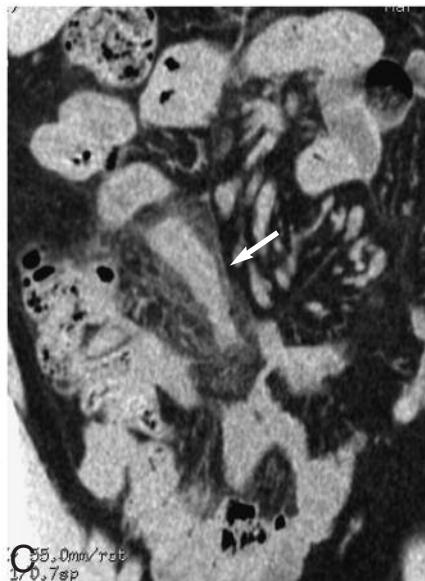
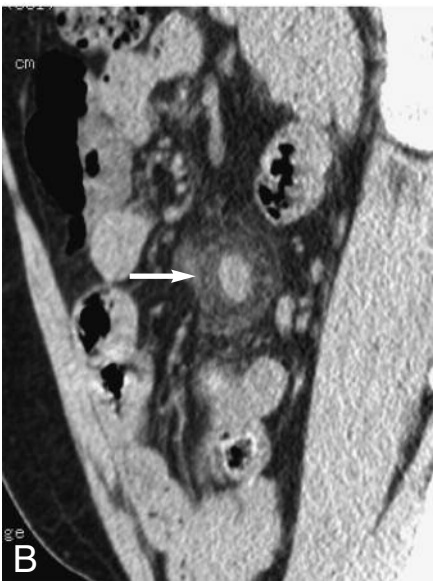
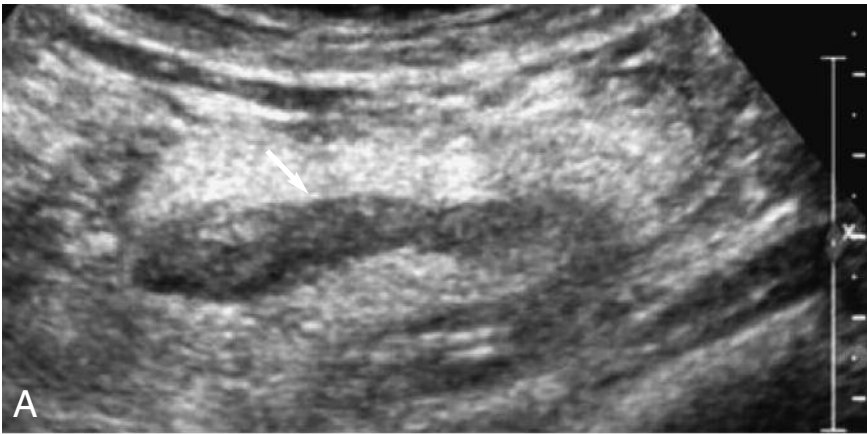


Fig. 5. — A 45-year-old patient presented with deep pain in the right iliac fossa. US (A) demonstrated a 5 cm digitiform hypoechoic structure (white arrow) surrounded by inflammatory plastron and first evocating atypical paracecal necrotic appendicitis. Unenhanced abdominal MDCT with sagittal (B) and coronal (C) MPR confirmed the ultrasound data. The hypothesis of appendicitis was rejected because the structure failed to join the cecum. Laparoscopy revealed a necrotic and hemorrhagic appendage. The hemorrhagic necrosis explained the unusual imaging findings.

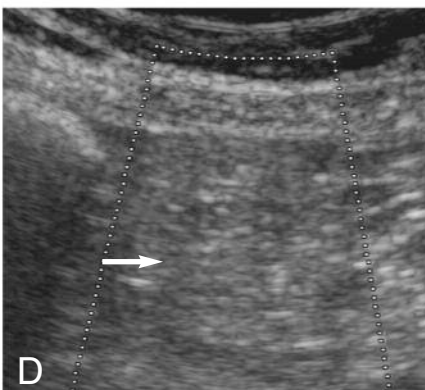
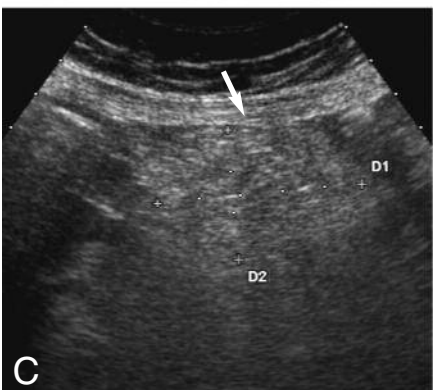
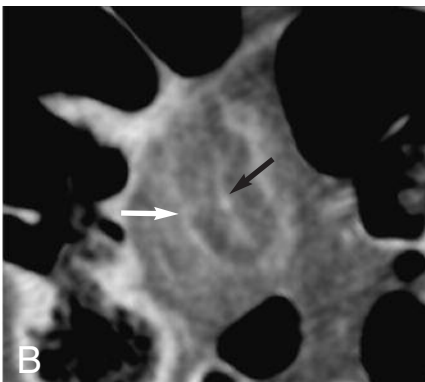
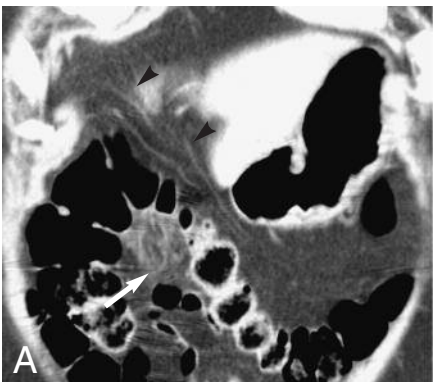


Fig. 6. — Atypical case of AEA of the right upper abdominal quadrant found in a 73-year old male (white arrows). On coronal MPR views (A, B) it is found hanging at the right angle of the colon (along the taenia libera). The thrombosed vascular pedicle is visible (black arrow); During ultrasound (C) with colour Doppler (D) the painful lesion is typically found nonvascular. It appears rather superficial, situated just under the abdominal wall because of the unusual prehepatic projection of the GO well identified through its vessels (black arrowheads on A). A spontaneous healing was obtained with conservative medical treatment.

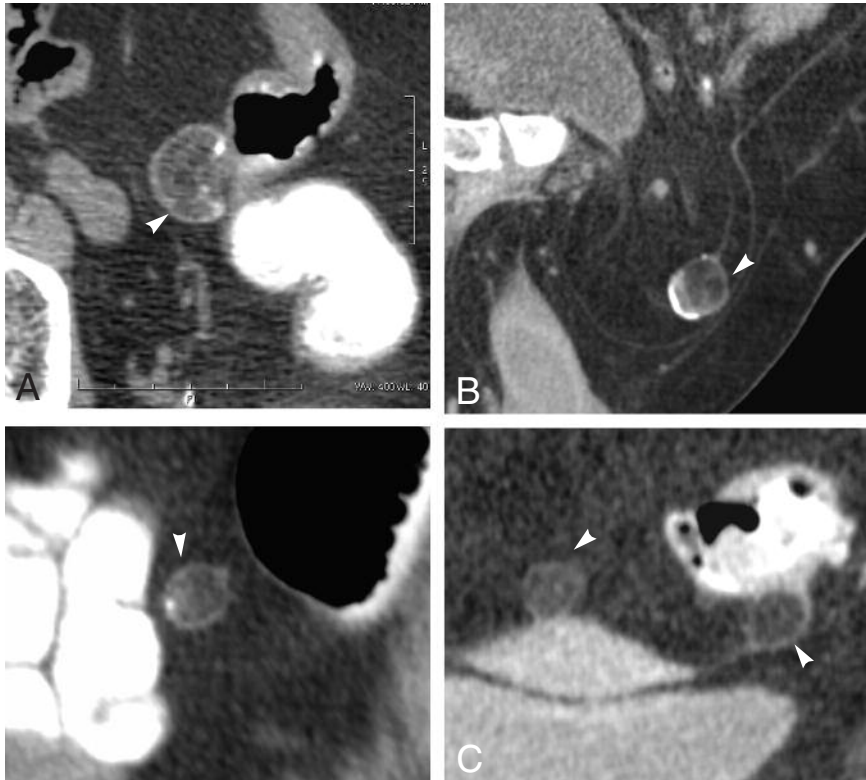


Fig. 7 — Subacute and chronic epiploic appendagitis (A-C) present as small lipomatous balls which are still attached to the colon (white arrowheads) or already free into the peritoneal cavity (black arrowheads). The diameter of the lesion is frankly inferior to the diameter encountered in the acute phase. The shape is more round and the neighbouring plastron has disappeared. Small foci of calcifications appear. On B the appendage has migrated into an inguinal hernia.

that usually ranges from 14 to 36 cm, it turns superiorly on itself to drape over the transverse colon and extend to the retroperitoneal pancreas (17). The descending and ascending portions usually fuse to form a four layer vascular fatty apron, with a space continuous with the lesser sac sometimes separating the two sets of layers (16, 17) (Fig. 10).

The GO is composed of a trabecular connective tissue framework that carries arteries, veins, lymphatics and fat pads (15). The arterial supply of the GO is determined by the right and left gastroepiploic arteries receiving their blood supply from the celiac trunk, the left one by the lineal artery and the right, a stronger one, from the gastroduodenal artery which in turn carries blood from the superior mesenteric artery (15). Both gastroepiploic arteries pass tortuously along the greater gastric curvature and decrease in diameter by giving off gastric and epiploic branches at a right/left ratio of 3:1. About 5 to 13 epiploic arteries originate from the right gastroepiploic

artery. Only one main epiploic artery emerges from the left gastroepiploic artery. These arteries descend mostly at right angles to the greater curvature and bifurcate close to the omental margin, where they eventually anastomose through small branches with adjacent epiploic arteries. The venous drainage parallels the arteries and empties into the portal system.

The identification of this rich vascular network and particularly that of the essentially vertical course of the epiploic vessels (particularly the veins which are generally twice as large as the arteries) constitutes the main landmark for current prompt identification of the GO during abdominal MDCT. These vessels may be clearly identified in 100% of patients (18) (Fig. 10).

The GO represents the most superficial fatty intraperitoneal apron and thus its free edge can be easily identified during scrupulous up and down cine view analysis of the MDCT axial views just at the level where the fatty omental apron abruptly disappears allowing the

intestines to lie directly beneath the abdominal wall (18).

Segmental omental infarction is a rare and uncommon acute disorder that simulates common surgical emergencies such as cholecystitis, appendicitis, or diverticulitis (16). Although omental infarctions have been reported in various portions of the GO most cases (90%) concern right-sided segmental infarction (19, 20). Left sided infarction is rare and only sporadically reported (21, 22). Due to the increasing use of US and CT and now MDCT evaluation in the setting of acute abdominal pain, infarction of the GO has gained much interest, especially because it may also be managed conservatively (1, 2, 19, 23).

The exact etiology and pathogenesis of acute pathology is unknown (2, 16, 20). Some authors have suggested that congenitally anomalous fragile blood supply to the right lower portion of the greater omentum renders this region prone to infarction (24). Other authors suggest a different embryonic origin for the right side of the greater omentum with more fragile blood vessels which are more susceptible to elongation and secondary occlusions (25). Variations in blood supply to the right omental edge associated with obesity or trauma, overeating, hypercoagulability, coughing or a sudden change in position have also been suggested as predisposing factors. Other authors suggest venous engorgement after heavy meals or venous elongation produced by excessive weight of the greater omentum as a cause of infarction, since the higher prevalence of the syndrome in the obese population.

Significant anatomic variations, some of which being related to sex, have recently been described during a 64-row MDCT study (18). These variations first concern the length, shape and the relative thickness of the GO. Among these variations, the projection of a less or more important portion of the GO into the pre-hepatic sub-phrenic space appears to be an almost exclusive male feature (32% in males versus 2% in females) and in patients presenting with this feature the epiploic vessels appear somewhat crooked around the falciform ligament on 3D reformations (Fig. 11, 12).

This anatomic variant may also explain the fact that omental infarction are first more common on the right but also more common in males (adult and children) than in

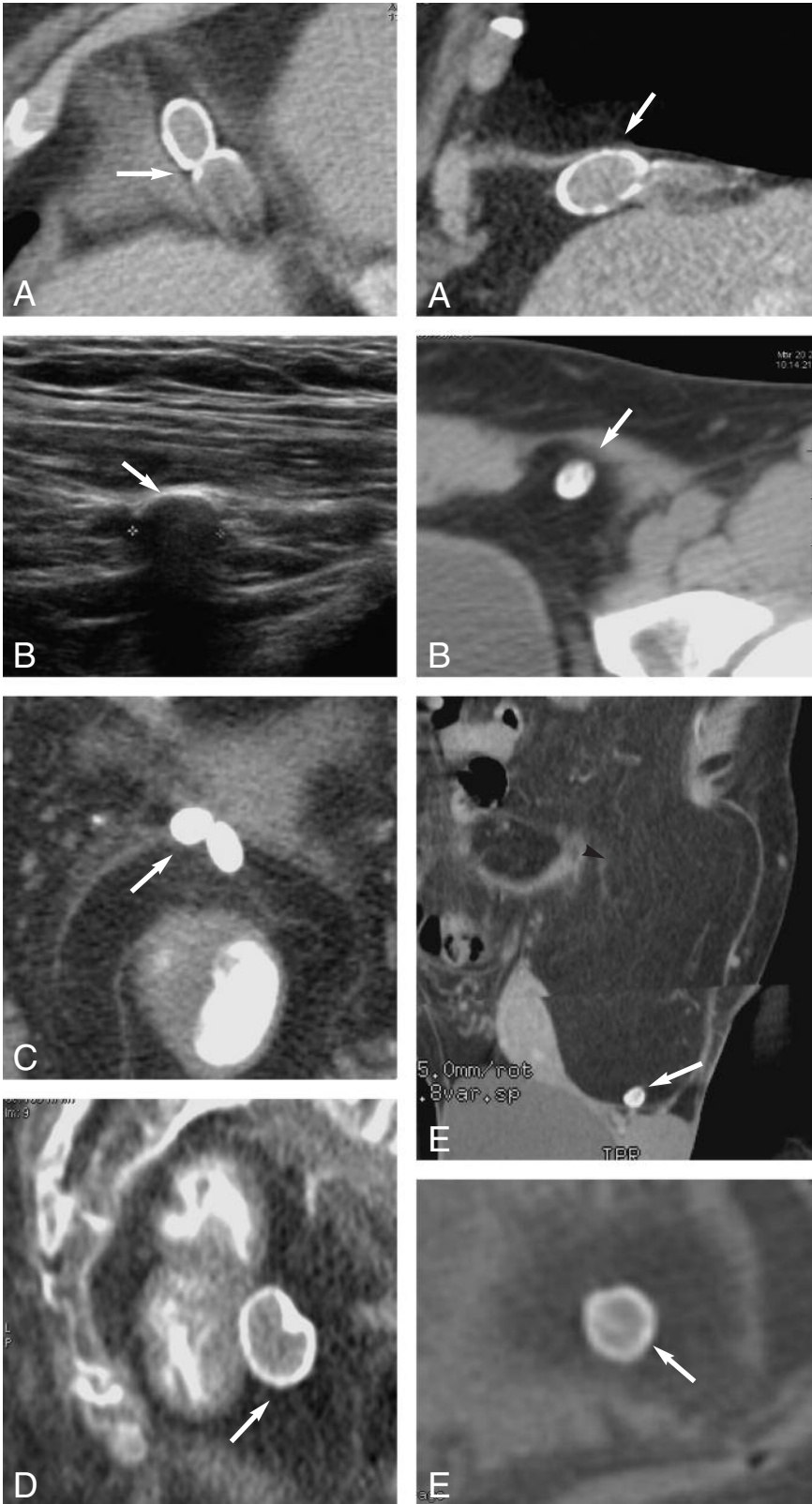


Fig. 8. — Calcified and detached endstage epiploic appendages (white arrows) may be secondarily retained in numerous recesses of the peritoneal cavity such as folds of the diaphragm above the liver dome (A), external inguinal fossa (b) (US and MDCT), the Douglas pouch (C, D) or in the bottom of a large inguinal hernia containing a large portion of the GO (E) (black arrowhead).

females with a sex ratio varying between 2:1 to 4:1 (18). It is possible that during exertion with increase of abdominal pressure or after heavy meals (predisposing situations that have been proposed in the pathogenesis of omental infarction) this vascular crooking increases leading to infarction or torsion. Is this subphrenic projection of the GO a permanent feature or only a transient phenomenon that disappears in upright position is a question that cannot be answered, all abdominal MDCT being performed on a supine patient.

Clinically, most patients present with acute or subacute abdominal pain. The pain may be to the left or right side of the midline based on the side of omental involvement. Pain may localize to the upper or lower quadrant of the abdomen, simulating acute appendicitis (66%) or cholecystitis. In female patients, the entity can also mimic gynecologic problems.

The physical findings are variable but usually there is tenderness in the right side of the abdomen, predominantly at the right lower quadrant. Physical examination usually elicits localized tenderness with or without a palpable "mass". Temperature is usually normal or slightly raised. Occasionally, the WBC count may be elevated. Therefore, clinically, omental infarction is difficult to be distinguished from appendicitis, cholecystitis, or adnexal problems (1, 2, 19, 20).

The histological appearance of omental infarction differs with the duration of insult. Initially, hemorrhagic infarction with fat necrosis is seen, followed by infiltration by lymphocytes, histiocytes, and finally, fibroblasts, resulting in fibrosis and scar formation (19, 20, 26).

The traditional classification of omental infarction without (primary infarction) or with (secondary infarction) torsion is clinically irrelevant because clinical findings imaging prognosis and treatment are the same (19, 20, 27).

Before the advent of cross sectional imaging, segmental infarction was rarely diagnosed before surgery.

Sonographically the classical presentation (1, 2, 19, 27, 28) consists of a solid, non-compressible, painful and moderately hyperechoic hyperattenuating mass in the vicinity of other abdominal structures. The lesion is typically found under the abdominal wall and covering the right colon (Fig. 12).

On CT the presentation is also that of a well circumscribed fatty

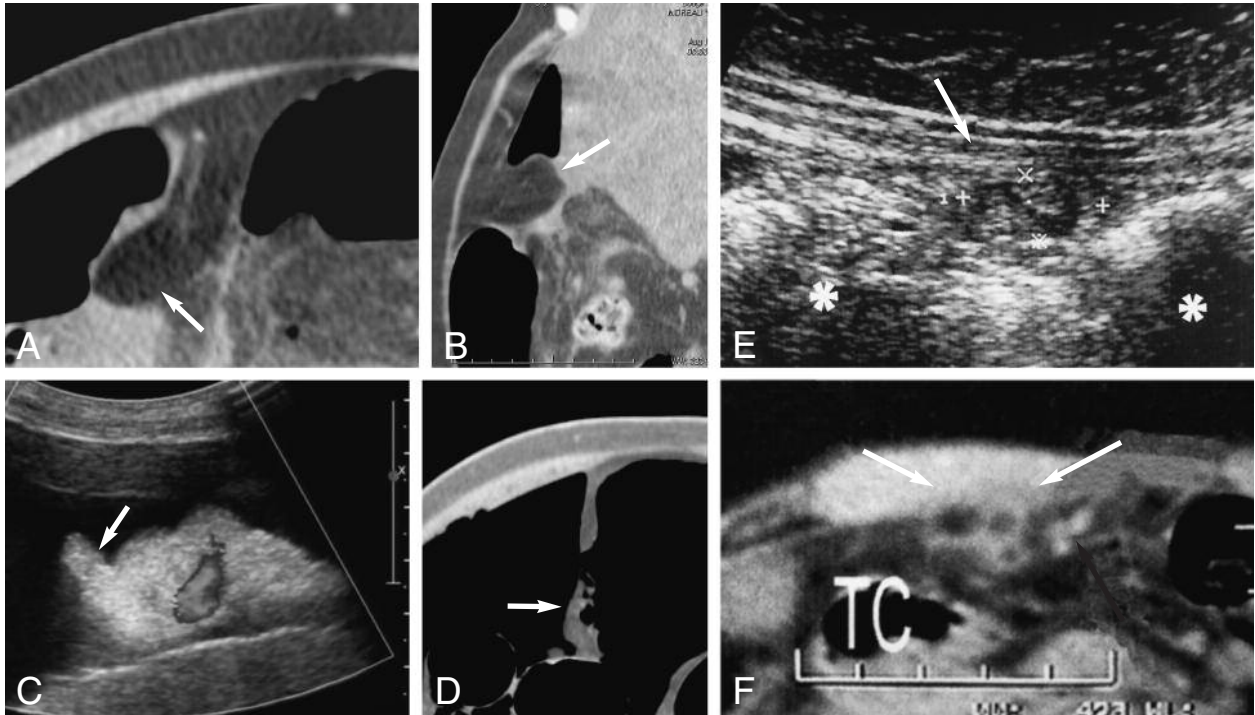


Fig. 9. — The normal falciform ligament is usually not visible unless surrounded by pneumoperitoneum (A, B, D) or ascitis (C). Lipomatous appendage are commonly hanging to the falciform ligament (white arrow on A-D). Sagittal US (E) and axial CT view (F) of a surgically proven infarcted lipomatous appendage of the falciform ligament found in a 25 year-old female presenting with epigastric pain. During ultrasound the small painful massa didn't move with the intestinal structures (white asterisk) proving its parietal fixation. It was situated just under the right rectus muscle. On CT the lipomatous necrotic massa (white arrows) was situated just near the ligamentum teres (black arrow); TC = transverse colon.

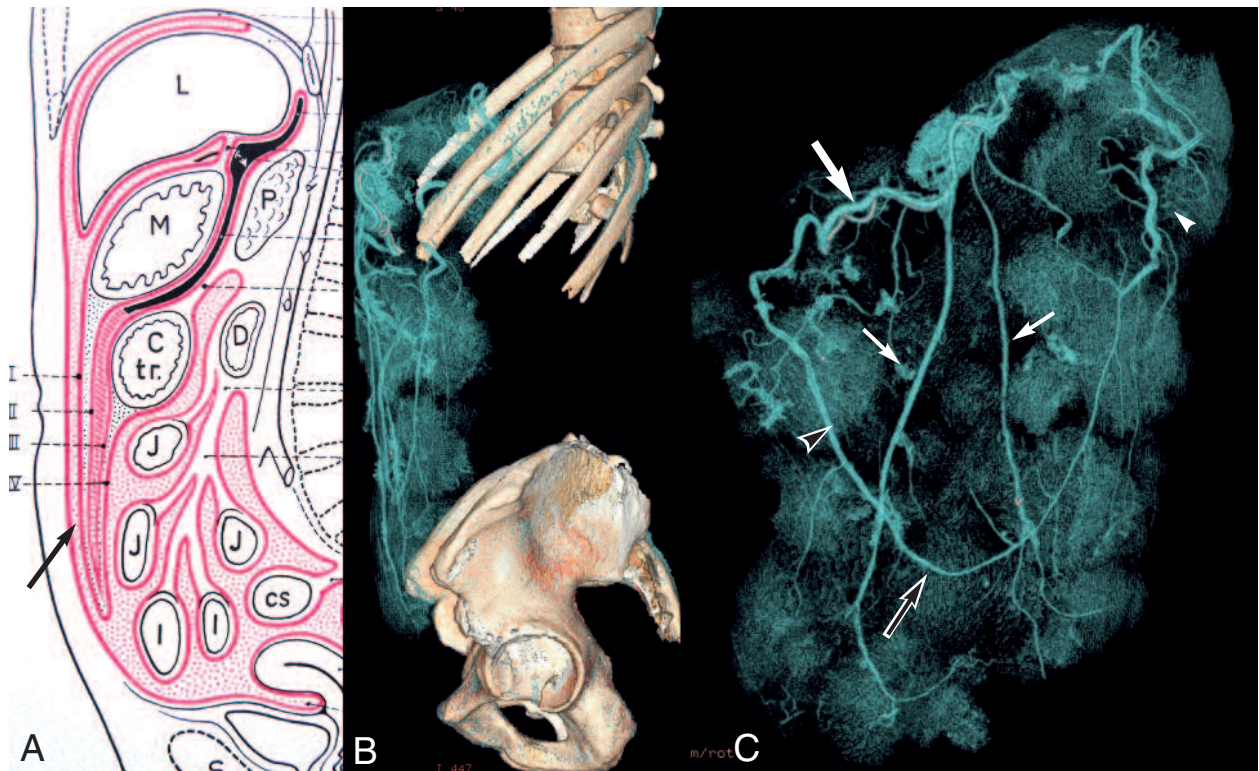


Fig. 10. — Classical sagittal schematic anatomy of the greater omentum (GO) and peritoneum compartments. The vertical hanging portion (black arrow) of the greater omentum is constituted by the fusion of the four layers of the inferior recess of the bursa omentalis. Corresponding sagittal MDCT VR view (B) of the GO in a 45 year-old female. Anteroposterior VR view (c) of the same GO illustrating the anatomy of the veins (which are essential for the CT identification of the GO) comprising main left (white arrowhead) and right (black arrowhead) omental veins, a variable amount of intermediate vertical veins (small arrows) and the arch of Barkow (black arrow) a frequently well distinguishable anastomosis between left and right omental veins.

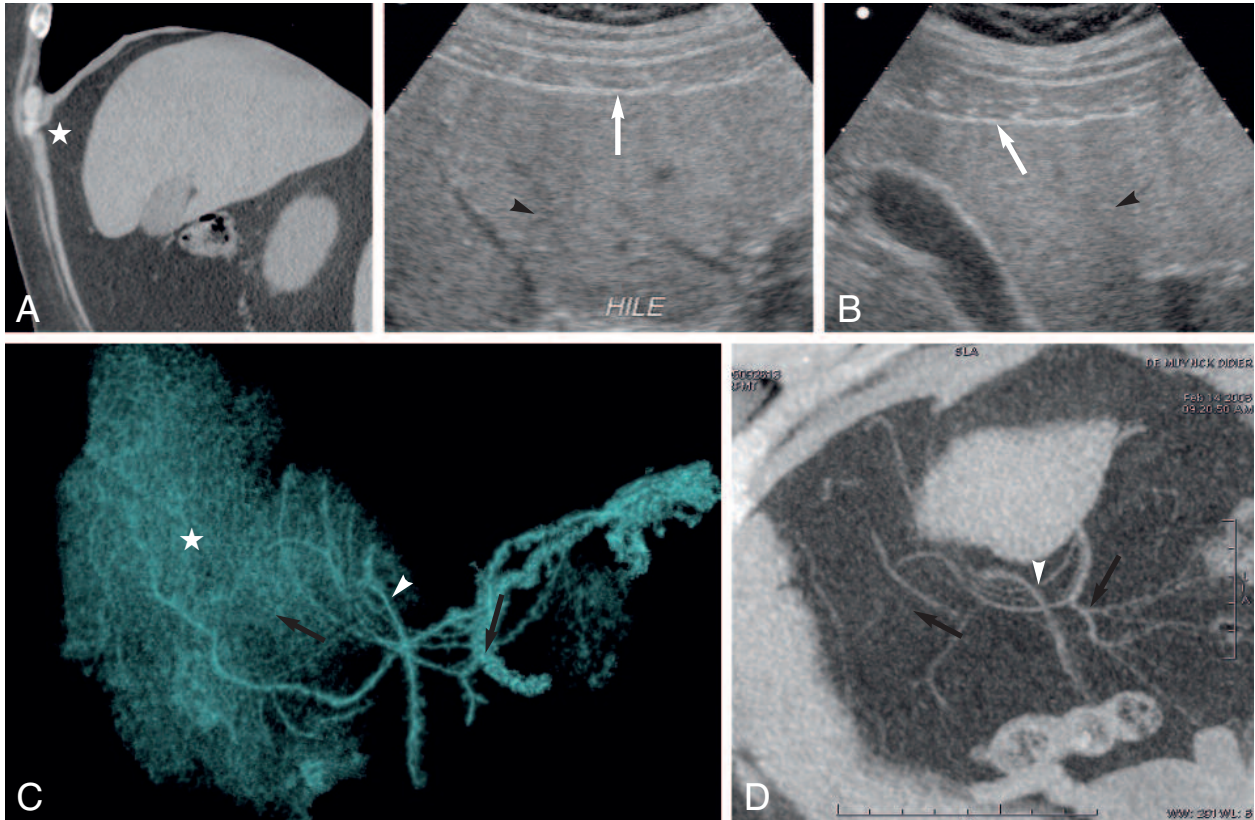


Fig. 11. — Details of the prehepatic subphrenic projection of the right portion of the GO in a 55 year old male. This sagittal MPR view (A) shows the prehepatic projection of the omentum (star). Right upper quadrant ultrasound (B) demonstrates the hepatic omental covering (white arrows) that induces linear artefacts disturbing the homogeneity of the liver during scanning. Selected VR (C) and sagittal oblique MIP view (D) illustrate the “crooking” of the epiploic vessels (black arrows) under the falciform ligament (white arrowhead). This “crooking” could favour infarction of the right portion of the GO.

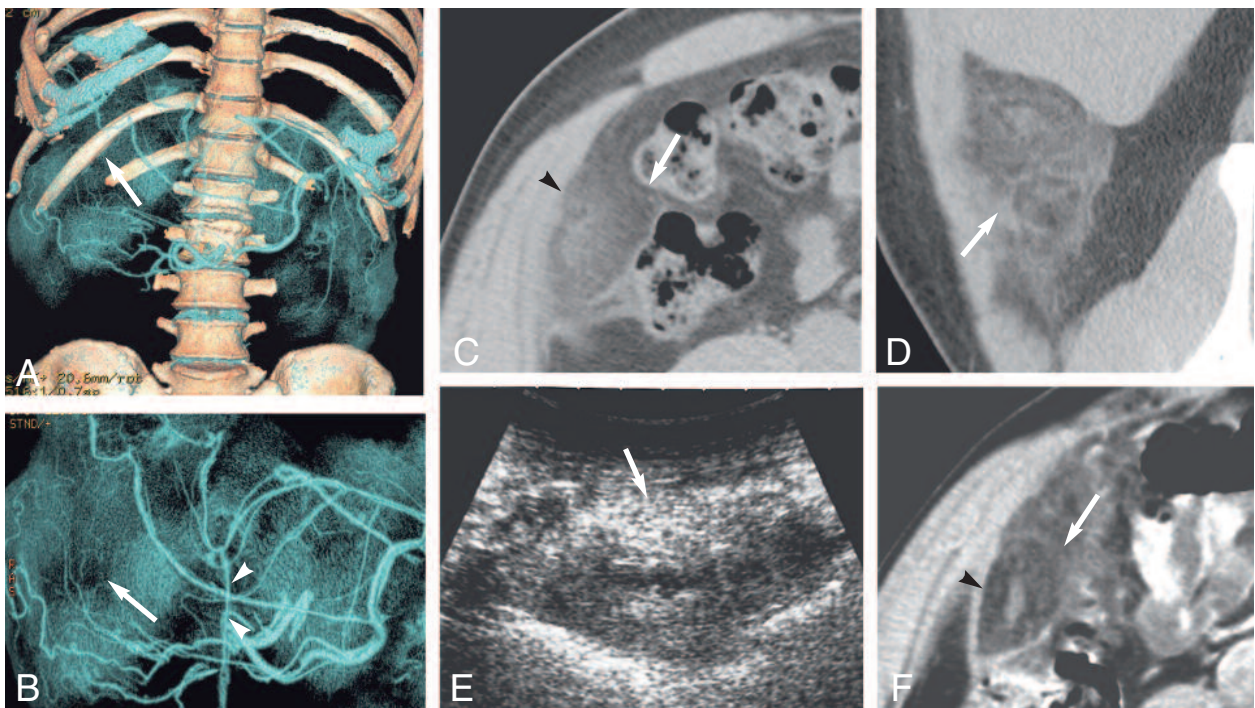


Fig. 12. — MDCT VR views (A, B) illustrating the subphrenic projection of the right portion of the GO (white arrow), an anatomic variant spontaneously found in 32% of the male population. This variant induces a severe “crooking” of numerous omental vessels under the falciform ligament (white arrowheads) and may contribute to explain the fact that omental infarction are more common in males and on the right.

Axial (C) and sagittal oblique MPR (D) views of a typical case of right sided infarction of the right greater omentum (white arrow). The peritoneum is clearly inflamed (black arrowhead) and it explains the clinical pain. US (E) and axial CT (F) of another similar case (white arrow) with massive thickening of the peritoneum (black arrowhead). Both patients were treated conservatively.

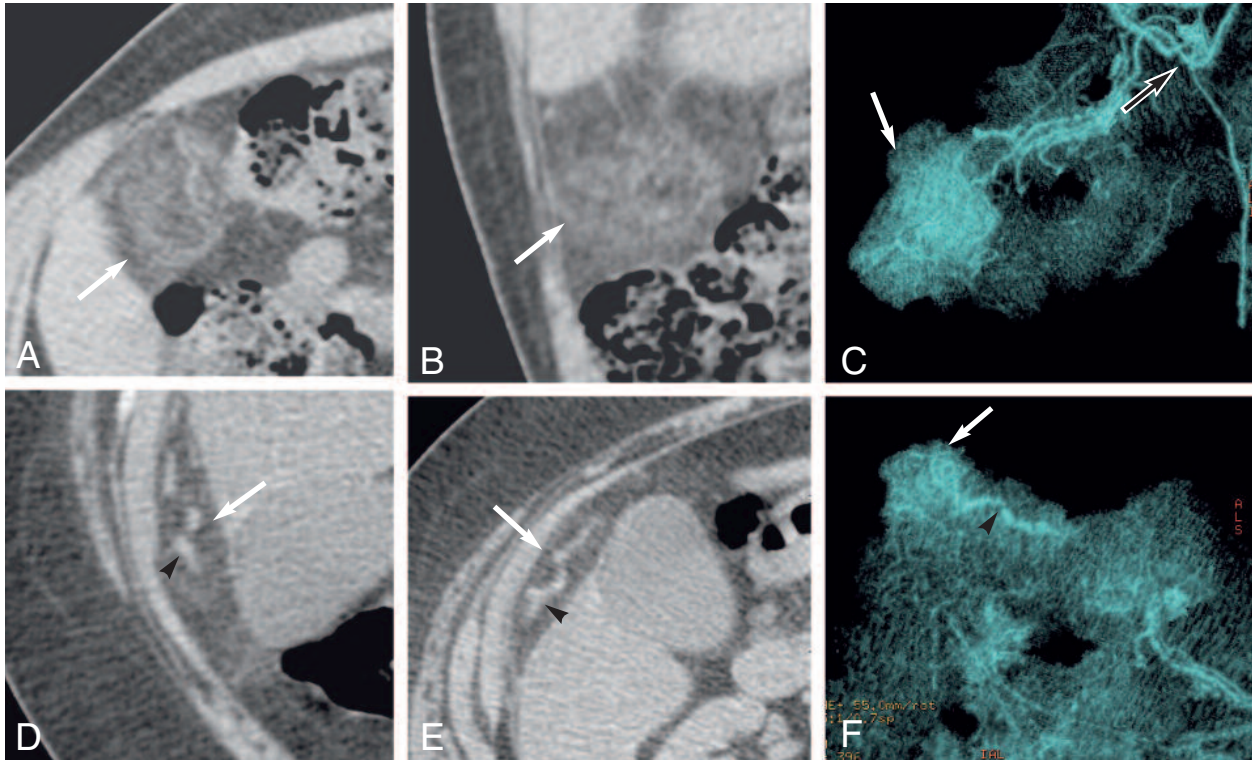


Fig. 13. — Axial (A) , coronal oblique (B) MPR views and selective VR view (C) of a typical case of right segmental infarction of the GO in a 60-year-old man. The lesion measures 4 x 4 cm and the vessels of the right portion of the GO are walking under the ligamentum teres of the falciform ligament (black arrow). Another case (D-F) of right segmental infarction (white arrows) of the GO in a 65-year-old female. Dense and probably thrombosed prominent veins are clearly seen (black arrowhead). These two patients were successfully treated conservatively.

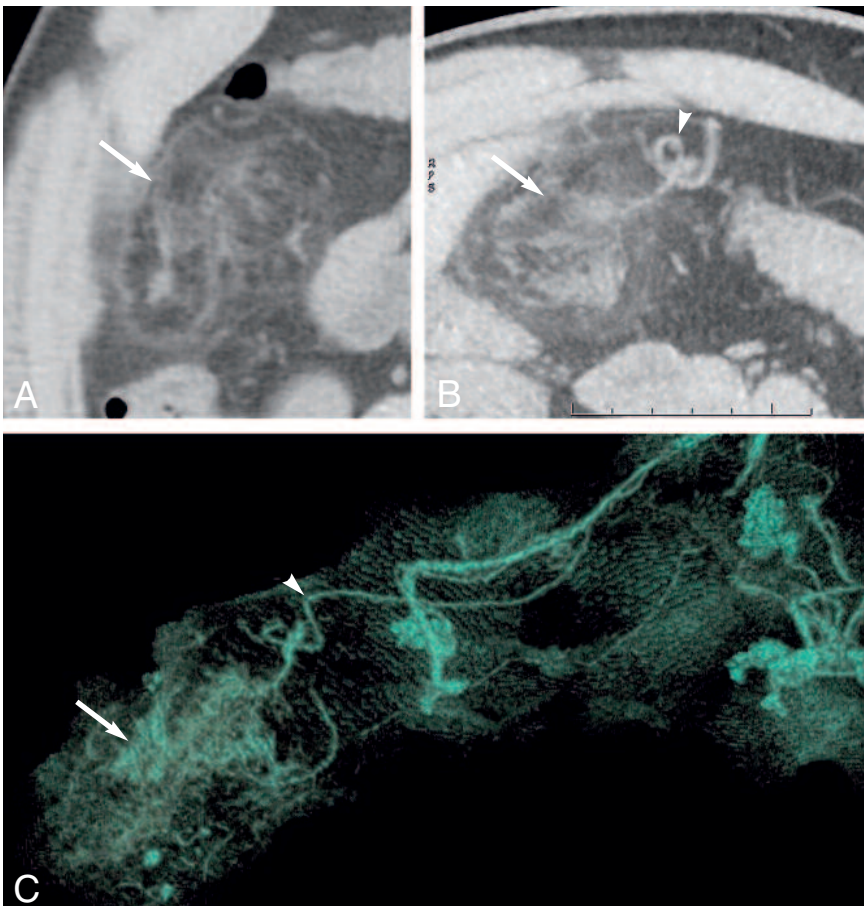


Fig. 14. — Coronal oblique (A) and axial (B) MPR views of a typical case of right segmental infarction (white arrow) of the GO in a 40-year-old man. The typical lesion measures 6 x 7 cm and contains irregular hemorrhagic foci and is surrounded by inflammatory peritoneum. Global selective VR view (C) of the greater omentum illustrating the right segmental infarction (white arrow). Axial oblique MIP view (D) and focused VR view (E) demonstrating a typical whirl of the epiploic vessels (white arrowheads) proving that the infarction was due to segmental torsion of the omentum. The patient was successfully treated conservatively.

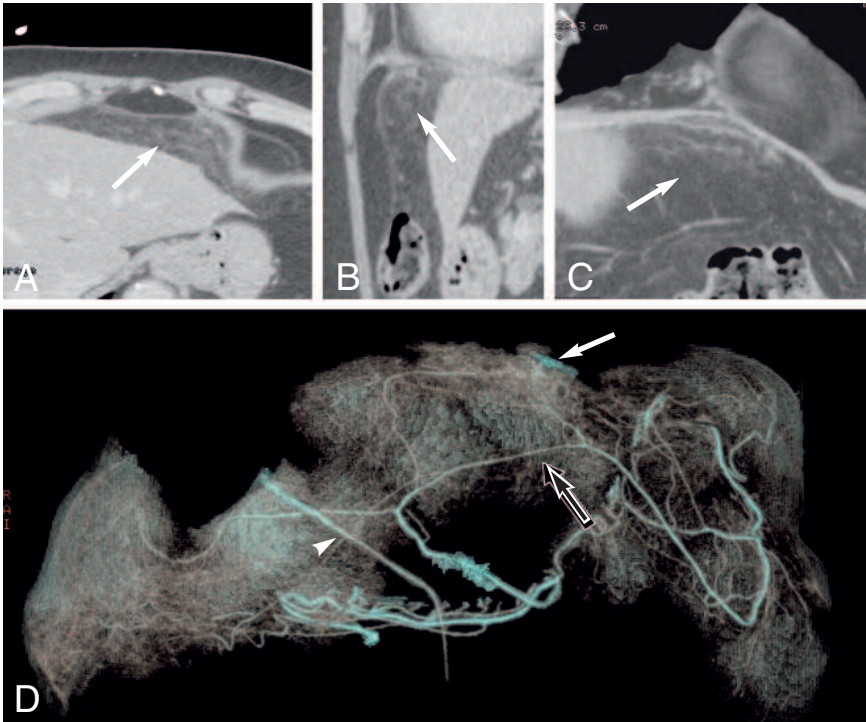


Fig. 15. — In this 50 year old patient presenting with medial subphrenic epigastric pain, axial (A), sagittal (B) and coronal (C) MPR views demonstrate the unusual segmental infarction of a portion of the free edge of the GO (white arrow). Volume rendering view (D) reveals that a complete coronal luxation of the GO has produced projecting its free edge in the subphrenic epigastric area. The displacement of the venous arch of Barlow illustrates the luxation (black arrow). White arrowhead = falciform ligament.

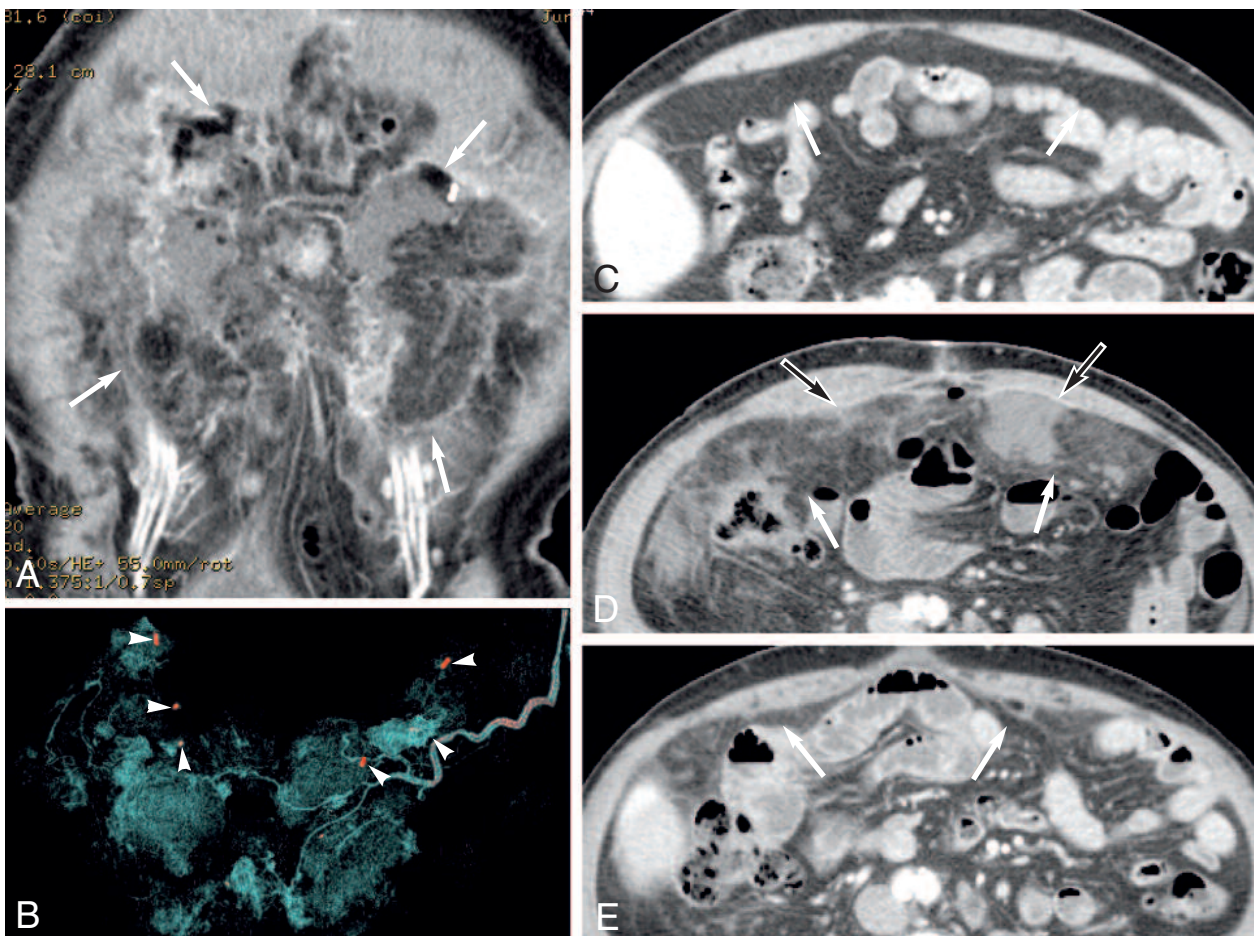


Fig. 16. — Massive infarction of the nearly entire greater omentum (GO) found in a 73 year old patient after total gastrectomy. During surgical dissection numerous epiploic vessels were clipped. In the postoperative period the patient developed diffuse and heavy abdominal pain. Coronal (A) and axial (D) MPR views demonstrate a diffusely heterogeneous swollen and dedifferentiated swollen GO (white arrows) intermingled with necrotic fluid collections. The recovering peritoneum was sharply thickened (black arrows). Selective VR view (B) of the necrotic GO clearly shows the row of surgical clips (white arrowheads) responsible of the necrosis. The patient was treated conservatively. Abdominal CT return to normal in two months. The only consequence was a severe atrophy of the GO (E) when compared with the preoperative CT (C).

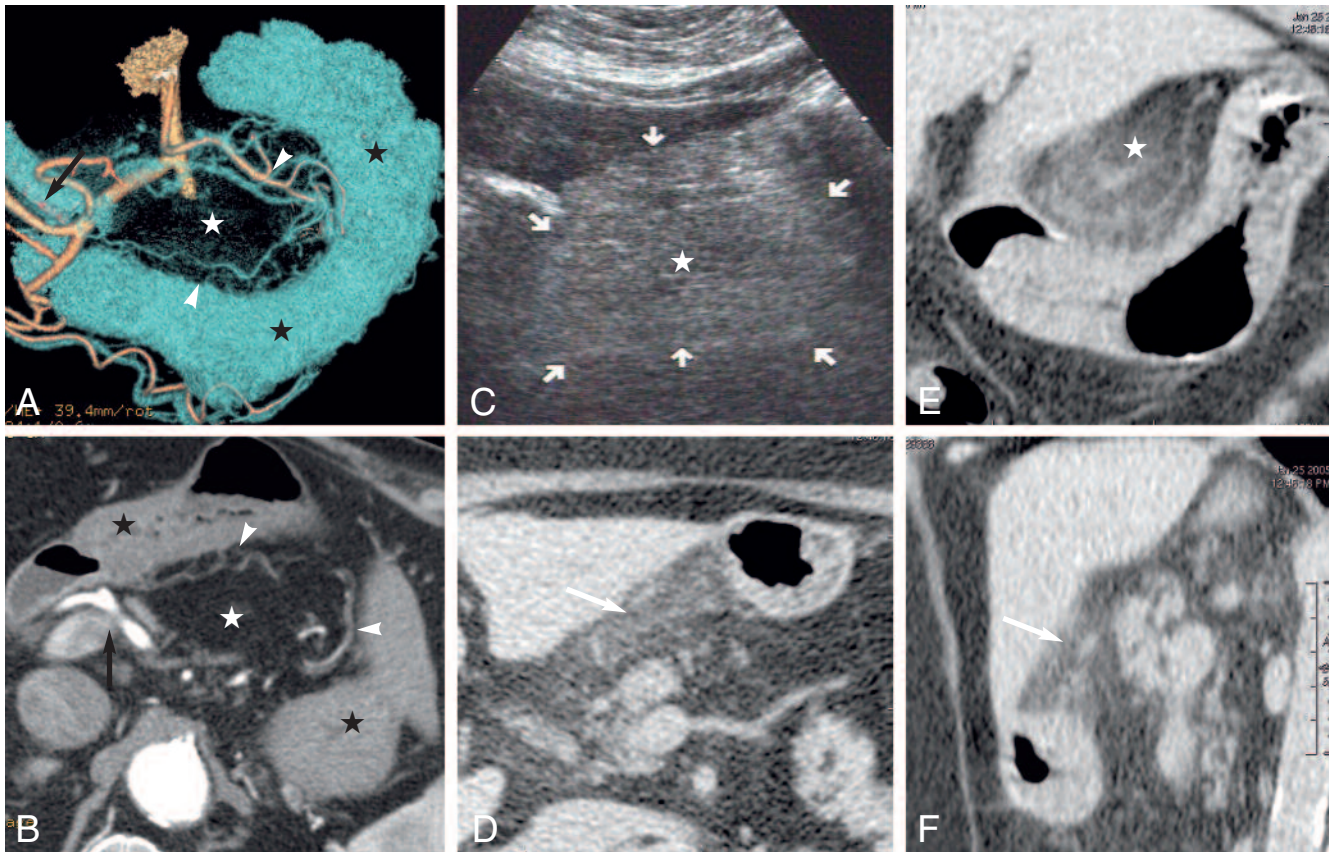


Fig. 17. — Selective volume rendering (A) and axial oblique (B) MPR views of the normal lesser omentum. This fatty ligament (white star) inserts along the lesser curvature of the stomach (black star) and its peripheral border contains the left and right gastric vessels (white arrowheads). Its right free edge contains the hepatic vessels (black arrow). A rare case of lesser omentum (white star) infarction diagnosed in a 72-year old obese woman (A, B). Transversal US view (C) of the epigastric area shows a 5 x 4 x 3 cm painful, incompressible hyperechoic mass (white arrows). Coronal oblique (E), axial (D) and sagittal (F) MPR views confirm that the inflammatory mass corresponds to the infarcted lesser omentum. The clinical evolution was spontaneously favourable.

inflammatory mass, surrounded by normal viscera, circumscribed or covered by an inflammatory peritoneum and containing hyperechoic streaks probably corresponding to fibrous band and/or dilated thrombosed veins (1, 2, 19, 26-29) (Fig. 12-16). Integrity of the adjacent organs eliminates the diagnosis of inflammatory fat secondary to more classical conditions such as diverticulitis, appendicitis, cholecystitis and Crohn disease. In rare cases an associated thickening of the transverse colon at the level of the insertion of the infarcted GO may be seen (19, 30).

The presence of concentric linear streaks at the level of the torsion site is considered as pathognomonic for an omental torsion but this sign as been extremely rarely described (2, 30-33). Thanks to its high capabilities of millimetric MPR, MDCT would probably be able to better demonstrate torsion of epiploic vessels (Fig. 14).

Because of the good prognosis and spontaneous favourable evolu-

tion is most cases, follow-up studies are not systematically performed and in the very rare cases in which follow-up was available, complete resolution on inflammatory changes of both omentum and peritoneum was documented (2) (Fig. 16).

Finally very rare cases of traumatic omental infarction (34, 35) (Fig. 19) and of twisting and infarction of the entire greater omentum have also sporadically been reported (36).

It is well now recognized that the diagnosis of IFFI is safer with CT than with US, not only because the signs are more consistent and specific but also because CT generally definitively more safely excludes other mimicking or associated acute inflammatory abdominal conditions (1, 28).

Lesser omentum

The lesser omentum, which is a combination of the gastrohepatic and hepatoduodenal ligaments, connects the lesser curvature of the stomach and proximal duodenum

with the liver and covers the lesser sac anteriorly.

This frontal peritoneal meso is constituted of two folds -anterior and posterior- and four borders - hepatic, gastric, superior and a free right border-. The thickness is variable being slim in the middle area near the gastric insertion (pars flaccida), thicker in the oesophageal superior portion (condensed pars containing vessels) and in the right duodenal portion (duodeno-hepatic pars).

The left portion (or gastrohepatic ligament) contains the left gastric vessels and left gastric lymph nodes and the right portion (or hepatoduodenal ligament) contains the portal vein, hepatic artery, extrahepatic bile duct, and hepatic nodal group (16, 37, 38).

Primary masses or neoplasms of the lesser omentum are rare and include benign tumors (lymphangioma, neurogenic tumor, teratoma) and malignant neoplasms (liposarcoma, malignant gastrointestinal stromal tumor). Almost all of these

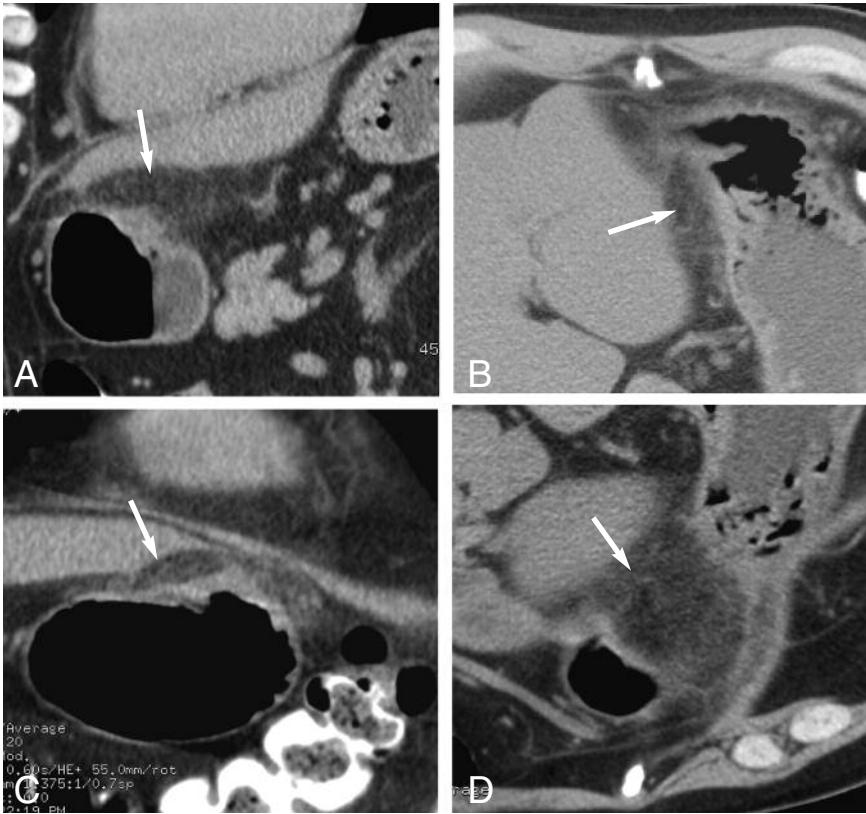


Fig. 18. — Sagittal (A), axial (B), coronal (C) and oblique (D) MPR views of the epigastric area obtained in a 54-year-old patient presenting with unusual epigastric pain amplified during deep inspiration. Ultrasonography (not illustrated) was uncontributive but unenhanced MDCT revealed oedema and inflammatory changes of the anteroinferior portion of the lesser omentum. A segmental infarction of the lesser omentum was diagnosed. The evolution was spontaneously resolvable in a few weeks.

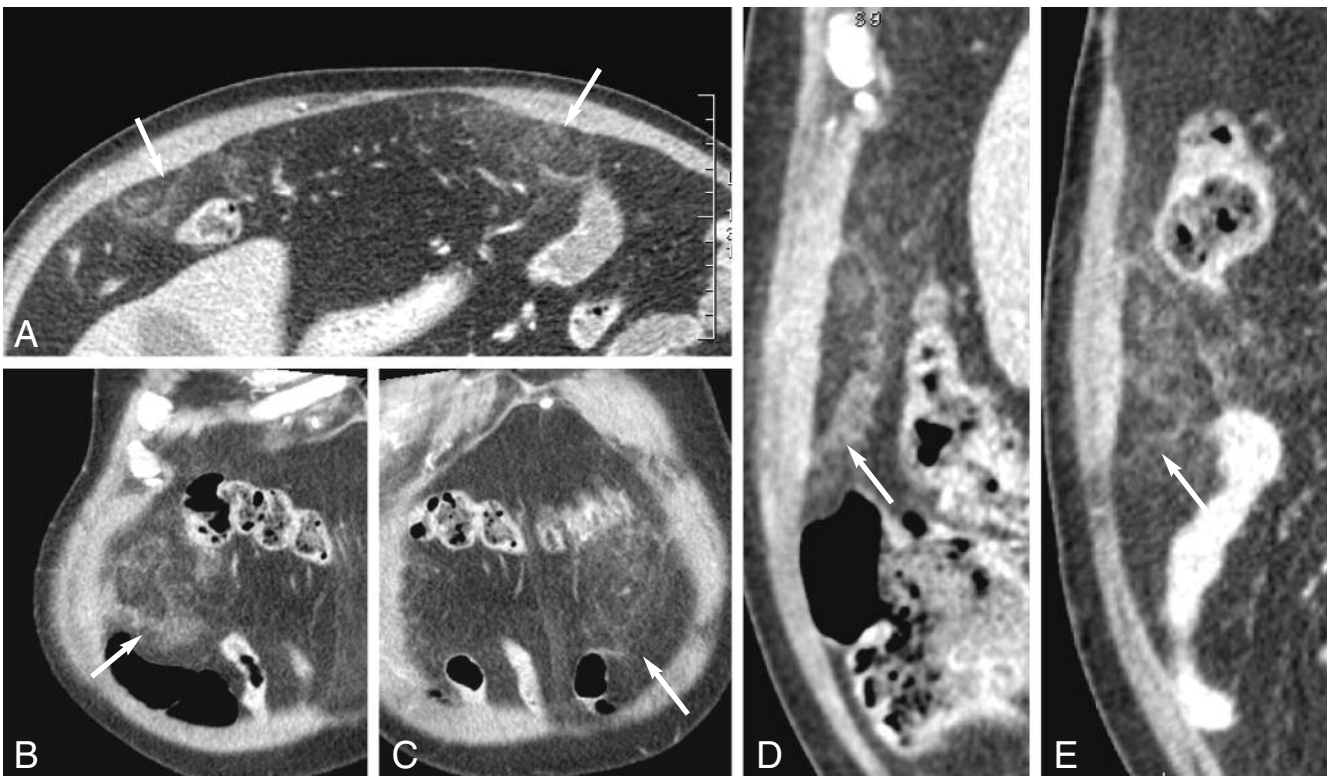


Fig. 19. — Unusual case of traumatic IFFI of the greater omentum diagnosed in a 70-year-old obese man. The patient was admitted with abdominal pain after a car accident during which he had received the steering wheel in the abdomen. Axial view (A) coronal oblique (B, C) and right and left sagittal (D, E) MPR views demonstrate foci of fat necrosis of the greater omentum (white arrows).

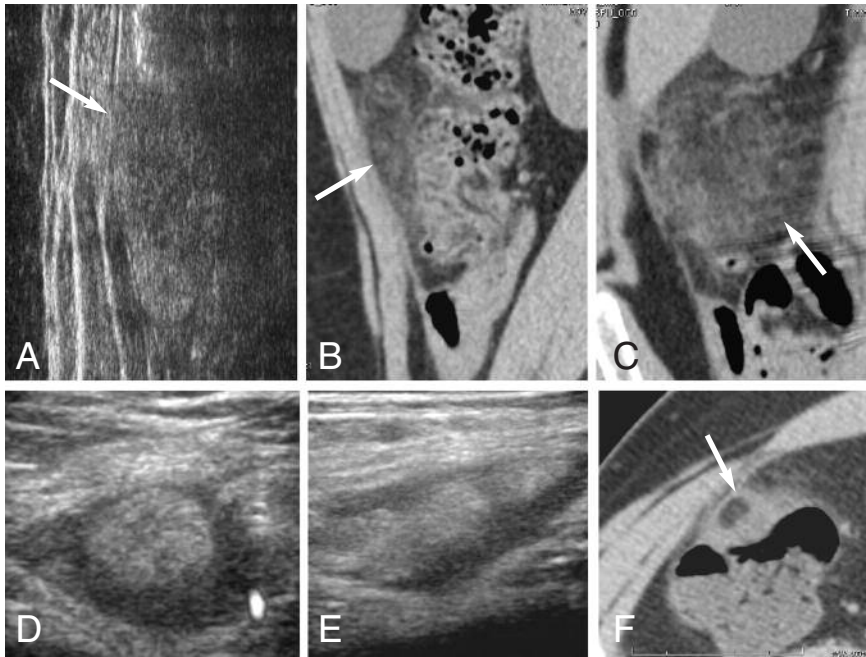


Fig. 20. — A rare case of segmental infarction of the GO (A-C) diagnosed in a 10-year-old obese boy: sagittal US view of the right flank (A) shows a 6 x 4 x 3 cm painful and incompressible precolic hyperechoic mass (white arrows). Corresponding sagittal oblique (B) and coronal (C) MPR CT views clearly identify a segmental infarction of the GO. Axial (D) and sagittal US (E) view and corresponding axial CT view (F) of a typical paediatric epiploic appendagitis (white arrow) of the right colon diagnosed in a 8-year-old boy. In the two cases the evolution was spontaneously favourable under medical treatment and the typical imaging findings revealed of primordial importance to exclude appendicitis and avoid unnecessary surgery.

tumors have variable and nonspecific CT features (16, 37, 38).

A review of the medical literature (Medline) also essentially reveals the implication of the lesser omentum in metastatic disease (lymphoma, lung and oesogastric tumours), portal hypertension (varicose) and mechanical hernias through the hiatus of Winslow.

Except for the location in the epigastric area, the rare reported cases of infarction of the lesser omentum presented with extremely similar findings in terms of clinical presentation, laboratory tests, US and CT findings with other reported IFFI cases (Fig. 17, 18). The differential diagnosis was to be made with gastro-duodenal ulcer disease and pancreatitis (37, 38).

Paediatric cases

AEA is generally found mostly in adults but about 15% of patients presenting with segmental infarction of the essentially right portion of the GO may be children (27, 28, 39, 40) and boys are affected twice as frequently as girls (Fig. 20). Like in adults the precise aetiology remains

controversial but obesity is a predisposing factor. Clinical and imaging features are the same as for adults. Notwithstanding the fact that the differential diagnosis of segmental omental infarction in children essentially concerns appendicitis and therefore more restricted than in adults, this clinical entity remains difficult to diagnose and in the most recent paediatric surgical papers surgery continues to be proposed as the treatment of choice (27, 39, 41, 42). There are several reasons to explain this discrepancy: firstly appendicitis remains the cardinal diagnosis in children presenting with acute right iliac fossa symptoms and in most cases the decision to perform appendectomy remains predominantly based on clinical signs only. Secondly for a justified question of radioprotection, US remains the primary imaging method in children and although specific in the diagnosis of omental infarction it has been shown to be not as sensitive as CT and extremely operator dependant (43). Surgeons also justify that the child's symptoms resolve rapidly after surgery and that

potential complications such as abscess formation or adhesions are minimised. These arguments are questionable and controversial (27, 44).

Unenhanced CT has been proposed in obese children who are more prone to present idiopathic omental infarction and in whom the diagnosis of appendicitis is clinically and sonographically invariably more difficult to establish (Fig. 20).

Bibliography

1. van Breda Vriesman A.C., Lohle P.N., Coerkamp E.G., Puylaert J.B.: Infarction of omentum and epiploic appendage: diagnosis, epidemiology and natural history. *Eur Radiol*, 1999, 9: 1886-1892.
2. Barbier C., Pradoura J.M., Tortuyaux J.M., et al.: Imaging of Segmental Infarction of the Greater Omentum: Diagnostic Findings and Pathophysiological Considerations. *J Radiol*, 1998, 79: 1367-1372.
3. Singh A.K., Gervais D.A., Hahn P.F., Rhea J., Mueller P.R.: CT Appearance of Acute Appendagitis. *AJR*, 2004, 183: 1303-1307.
4. Ghabremani G.G., White E.M., Hoff F.L., et al.: Appendices epiploicae of the colon: radiologic and pathologic features. *Radiographics*, 1992, 12: 59-77.
5. Sand M., Gelos M., Bechara F.G., et al.: Epiploic appendagitis - clinical characteristics of an uncommon surgical diagnosis. *BMC Surgery*, 2007, 7: 11.
6. van Breda Vriesman A.C., de mol van Otterloo J.C., Puylaert J.B.: Epiploic appendagitis: an underestimated self-limiting acute abdominal condition. *Ned Tijdschr Geneesk*, 2003, 147: 1113-1118.
7. Danielson K., Chemin J.R., Amberg J.R., Goff S., Durham J.R.: Epiploic appendagitis: CT characteristics. *J Comput Assist Tomogr*, 1986, 10: 142-143.
8. Rioux M., Langis P.: Primary epiploic appendagitis: clinical, US, and CT findings in 14 cases. *Radiology*, 1994, 191: 523-526.
9. Rao P.M., Wittenberg J., Lawrason J.N.: Primary epiploic appendagitis: evolutionary changes in CT appearance. *Radiology*, 1997, 204: 713-717.
10. Lloyd T.: Primary torsion of the falciform ligament: computed tomography and ultrasound findings. *Australas Radiol*, 2006, 50: 252-254.
11. Coulier B., Broze B., Mailleux P., Maldague P.: Small-bowel internal herniation through the falciform ligament: 64 row-MDCT diagnosis. *Emerg Radiol*, 2009, 28.
12. Brock J.S., Pachter H.L., Schreiber J., Hofstetter S.R.: Surgical diseases of the falciform ligament. *Am J Gastroenterol*, 1992, 87: 757-758.
13. Kakitsubata Y., Nakamura R., Shiba T., et al.: Lipoma of the falciform liga-

- ment: US, CT and MRI appearances. *Clin Imaging*, 1993, 17: 27-29.
14. Coulier B., Cloots V., Ramboux A.: US and CT diagnosis of a twisted lipomatous appendage of the falciform ligament. *Eur Radiol*, 2001, 11: 213-215.
 15. Liebermann-Meffert D.: The greater omentum. Anatomy, embryology, and surgical applications. *Surg Clin North Am*, 2000, 80: 275-293.
 16. Yoo E., Kim J.H., Kim M.J., et al.: Greater and lesser omenta: normal anatomy and pathologic processes. *Radiographics*, 2007, 27: 707-720.
 17. Sompayrac S.W., Mindelzun R.E., Silverman P.M., Sze R.: The greater omentum. *AJR*, 1997, 168: 683-687.
 18. Coulier B.: 64-row MDCT review of anatomic features and variations of the normal greater omentum. *Surg Radiol Anat*, 2009, 31: 489-500.
 19. Coulier B., Pringot J.: Pictorial essay. Infarction of the greater omentum: can US and CT findings help to avoid surgery? *JBR-BTR*, 2002, 85: 193-199.
 20. Battaglia L., Belli F., Vannelli A., et al.: Simultaneous idiopathic segmental infarction of the great omentum and acute appendicitis: a rare association. *World J Emerg Surg*, 2008, 29: 30.
 21. Hirano Y., Oyama K., Nozawa H., et al.: Left-sided omental torsion with inguinal hernia. *World J Gastroenterol*, 2006, 12: 662-664.
 22. Aoun N., Nader L., Haddad-Zebouni S., Ghossain M., Akatcherian C.: Left segmental omental infarction in a child: conservative treatment. *Arch Pediatr*, 2006, 13: 1040-1042.
 23. van Breda Vriesman A.C., Puylaert J.B.: Omental infarction: a self-limiting disease. *AJR*, 2005, 184: 156-162.
 24. Sanchez J., Rosado R., Ramirez D., et al.: Torsion of the greater omentum: treatment by laparoscopy. *Surg Laparosc Endosc Percutan Tech*, 2002, 12: 443-445.
 25. Tolenaar P.L., Blast T.J.: Idiopathic segmental infarction of the omentum. *Br J Surg*, 1987, 74: 1182.
 26. Karak P.K., Millmond S.H., Neumann D., Yamase H.T., Ramsby G.: Omental infarction: report of three cases and review of the literature. *Abdom imaging*, 1998, 23: 96-98.
 27. Coulier B.: Segmental omental infarction in childhood: a typical case diagnosed by CT allowing successful conservative treatment. *Pediatr Radiol*, 2006, 36: 141-143.
 28. Abadir J.S., Cohen A.J., Wilson S.E.: Accurate diagnosis of infarction of omentum and appendices epiploicae by computed tomography. *Am Surg*, 2004, 70: 854-857.
 29. Mack P., Chellappa N., Sidhu D.S., Lyer N.K.: Acute omental infarction: a report of six cases. *Ann Acad Med Singapore*, 1989, 18: 710-712.
 30. Garant M., Pinsky M.F.: Resident's corner. Answer to case of the month 46. torsion and infarction of the greater omentum. *Can Assoc Radiol*, 1997, 48: 130-132.
 31. Kim J., Kim Y., Cho O.K., et al.: Omental torsion : CT features. *Abdom Imaging*, 2004, 29: 502-504.
 32. Ceuterick L., Baert A.L., Marchal G., Kerremans R., Geboes K.: CT diagnosis of primary torsion of greater omentum. *J Comput Assist Tomogr*, 1987, 11: 1083-1084
 33. Naffaa L.N., Shabb N.S., Haddad M.C.: CT findings of omental torsion and infarction: case report and review of the literature. *Clin Imaging*, 2003, 27: 116-118.
 34. Shields P.G., Chase K.H.: Primary torsion of the omentum in a jackhammer operator: another vibration-related injury. *J Occup Med*, 1989, 30: 892-894.
 35. Ramos C.T., Sammartano R.: Laparoscopic omentectomy for omental infarction after bicycle handlebar injury. *J Laparoendosc Adv Surg Tech A*, 2008, 18: 327-329.
 36. Coppin T., Lipky D.: Twisting and infarction of the entire greater omentum managed by laparoscopy: a report of two cases. *Acta Chir Belg*, 2006, 106: 215-217.
 37. Coulier B., Van Hoof M.: Intraperitoneal fat focal infarction of the lesser omentum: case report. *Abdom Imaging*, 2004, 29: 498-501.
 38. Coulier B.: A new case of intraperitoneal fat focal infarction (IFFI) of the lesser omentum. *Eur Radiol*, 2006, 16: 954-955.
 39. Sakkellaris G., Stathopoulos E., Kafousi M., et al.: Primary idiopathic segmental infarction of the greater omentum: two cases of acute abdomen in childhood. *J Pediatr Surg*, 2004, 39: 1264-1266.
 40. Van Kerkhove F., Coenegrachts K., Steyart L., et al.: Omental infarction in childhood. *JBR-BTR*, 2006, 89: 199-200.
 41. Grattan-Smith J.D., Blews D.E., Brand T.: Omental infarction in pediatric patients: sonographic and CT findings. *AJR*, 2002, 178: 1537-1539.
 42. Varjavandi V., Lessin M., Kooros K., et al.: Omental infarction : risk factors in children. *J Pediatr Surg*, 2003, 38: 233-235.
 43. Schlesinger A.E., Dorfman S.R., Braveman R.M.: Sonographic appearance of omental infarction in children. *Pediatr Radiol*, 1999, 29: 598-601.
 44. Fragoso A.C., Pereira J.M., Estevo-Costa J.: Nonoperative management of omental infarction: a case report in a child. *J Pediatr Surg*, 2006, 41: 1777-1779.
-